Spintronic Oscillator Based on Spin-Current Feedback Using the Spin Hall Effect

Swapnil Bhuktare,* Hanuman Singh, Arnab Bose, and Ashwin. A. Tulapurkar
Department of Electrical Engineering, Indian Institute of Technology-Bombay, Powai, Mumbai 400076, India

(Received 25 August 2016; revised manuscript received 18 December 2016; published 27 January 2017)

We propose a radio-frequency nano-oscillator based on feedback of spin current into a magnetic tunnel junction (MTJ) with an in-plane magnetized pinned layer and an out-of-plane magnetized free layer. The MTJ is connected to a "feedback" strip of a material like tungsten with a giant spin Hall effect. On passing a dc current through the MTJ, the thermal fluctuations of its free layer produce an oscillatory voltage across itself owing to the magnetoresistance effect. This oscillatory voltage drives an oscillatory current into the tungsten strip which converts this charge current into spin current via the spin Hall effect and feeds it back to the MTJ. We show that this feedback can amplify the fluctuations further and drive the free layer into periodic precessional states. We also propose a way of implementing spin-current feedback by using a nanomagnet coupled to the free layer of the MTJ by dipolar magnetic field.

DOI: 10.1103/PhysRevApplied.7.014022

I. INTRODUCTION

A magnetic-tunnel-junction (MTJ) device consists of two ferromagnetic layers—a pinned layer and a free layer—separated by a tunnel barrier. A dc current passing through the pinned layer gets spin polarized and exerts a torque on the free layer. This phenomenon of spin-transfer torque (STT) can be used to switch the magnetization of the free layer or to drive the magnetization into continuous oscillations [1–8]. Much research is under way in the area of spin-transfer nano-oscillators (STNOs), especially to reduce the dc current bias and improve the output power and quality factor of oscillations [9–14]. A radio-frequency (rf) oscillator with magnetic field feedback was recently proposed by Dixit *et al.* [15]. It was demonstrated experimentally that the oscillator possesses a quality factor of more than 10 000 [16]. This type of oscillator is most effective in a configuration where both the pinned and the free-layer magnetizations are in plane. For in-plane free-layer and out-of-plane free-layer geometries, the critical currents with just a STT effect are larger [17,18]. We show here that a spin-current-feedback scheme proves to be most efficient for such geometries. The importance of delayed feedback on auto-oscillators and their synchronization properties was emphasized by Tiberkevich *et al.* [19]. A delayed spin-current feedback has been studied by Khalsa *et al.* [20] theoretically and shown to reduce the critical current for oscillation and improve the quality factor. Recently, it was demonstrated experimentally by Tsunegi *et al.* [21]. All these studies were carried out for a vortex MTJ. Here, we consider a MTJ with uniformly magnetized free and fixed layers and show that the feedback itself can be used for driving free-layer magnetization into auto-oscillations. We also show how spin current can be fed back into the free layer by using the spin Hall effect and a nanomagnet coupled to the free layer of the MTJ by dipolar magnetic field.

In the feedback schemez proposed herein, we make use of two well-known effects: tunneling magnetoresistance (TMR) and the spin Hall effect. The spin Hall effect refers to the generation of transverse spin current from charge current because of the spin-orbit coupling. It is characterized by a parameter called the spin Hall angle, which is defined as the ratio of transverse spin-current density to the charge-current density [22,23]. This spin Hall effect is seen as an efficient source of spin current, and active research is being conducted to search for new materials with larger spin Hall angles [24–33]. Some transition metals like platinum, tantalum, and tungsten show to be very promising in this direction because of their large spin-orbit coupling [28–33]. We choose tungsten for this work, as it is a metal with one of the largest spin Hall angles reported [30,31]. If dc current passes through the MTJ, the oscillations of the free-layer magnetization convert into an oscillating current (or voltage) signal due to the TMR effect. The oscillating charge current, after a certain delay, passes through a W strip to generate oscillating spin current via the spin Hall effect. The oscillating spin current is then fed back to the free layer. The delay is chosen such that the feedback amplifies the free-layer oscillations. If the dc current is greater than a certain threshold value called the critical current, any small fluctuation of the free-layer magnetization can be amplified and periodic precessional states can be obtained.

II. PROPOSED DESIGN AND ANALYTICAL TREATMENT

The proposed oscillator is shown schematically in Fig. 1. The pinned-layer (FM2) magnetization of the MTJ is in

*Corresponding author.
swapnilbhuktare4@gmail.com

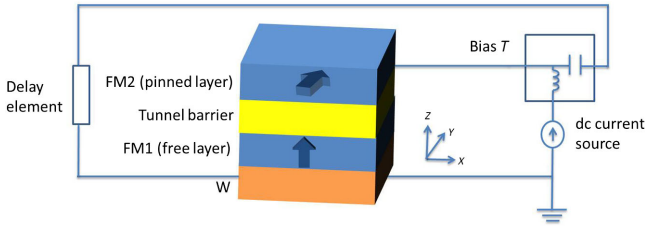

FIG. 1. Schematic diagram of the proposed spintronic oscillator. The top layer (FM2) is pinned along the y axis, and the bottom layer (FM1) is the free layer with an out-of-plane easy axis. The free layer is just above the W strip. Any fluctuation of the free-layer magnetization drives a fluctuating current through the W strip. The W strip converts this fluctuating charge current into spin current and feeds it back to the free layer. The delay element can be used to adjust the phase of feedback so as to amplify the oscillations of the free layer.

plane (taken along the y axis), and the free layer (FM1) magnetization in equilibrium is out of plane (the easy axis is along the z axis, and the in-plane hard axis is along the y axis). The MTJ rests on top of a W wire as shown in Fig. 1. We denote by L_x, L_y, t, and t_{W} the length, width, and thickness of the free layer and the thickness of the tungsten strip, respectively. The width of the tungsten strip is same as that of the MTJ, i.e., L_y.

The dynamics of the magnetization including the effect of the spin current is given by the Landau-Lifshitz-Gilbert-Slonczeski (LLGS) equation as

$$\frac{d\hat{m}}{dt} = -\gamma_0\,\hat{m}\times(\vec{H}_{\mathrm{eff}}+\vec{h}_r) + \alpha\left(\hat{m}\times\frac{d\hat{m}}{dt}\right) + \hat{m}\times\frac{\vec{I}_s}{qN_s}\times\hat{m}, \tag{1}$$

where γ_0 is the gyromagnetic ratio, $\vec{H}_{\mathrm{eff}}$ is the effective magnetic field comprising the external field and the anisotropy field, $\vec{h}_r$ is the random magnetic field arising because of the thermal fluctuations, α is the Gilbert damping constant, I_s is the spin current in units of charge current, q is the electronic charge, and N_s is the total number of spins given by $N_s = M_s V/\mu_B$ where M_s and V are the saturation magnetization and the volume of the free layer, respectively, and μ_B is the Bohr magneton. $\hat{m}$ denotes the unit vector along the magnetization direction. The first term in the above equation represents precession, the second term damping, and the third term is the STT term, which presents the action of the spin current. Assuming an external magnetic field along the z axis and the anisotropies in the y and z directions to be $H_{//}$ and $H_\perp$, respectively, the effective magnetic field $\vec{H}_{\mathrm{eff}}$ is given as $\vec{H}_{\mathrm{eff}} = -H_{//}m_y\hat{y} + (H_{\mathrm{ext}} + H_\perp m_z)\hat{z}$. We assume both $H_\perp$ and $H_{//}$ to be positive, which makes the z axis the easy axis and the y axis the hard axis. The random magnetic field $\vec{h}_r$ satisfies the properties

$$\langle h_{r,i}(t)\rangle = 0, \qquad \langle h_{r,i}(t)h_{r,j}(s)\rangle = 2D\delta_{ij}\delta(t-s)$$
$$\text{and} \quad D = \frac{\alpha k_B T}{\gamma_0\mu_0 M_s V}, \tag{2}$$

where k_B is the Boltzmann constant and T is the temperature.

The spin current in the last term in Eq. (1) has contributions from the spin current generated by the fixed layer due to the flow of dc bias current and spin current fed back into the free layer. The first contribution gives rise to a slight tilting of the free-layer magnetization and is, therefore, neglected in the following treatment. We show below that the second contribution gives rise to oscillations of the free-layer magnetization. Further, the oersted magnetic field produced by the current flow in the W strip (feedback magnetic field) can be shown to be much smaller than the spin-current-feedback effect (see the Supplemental Material [34]) and is neglected.

Now we calculate how much spin current is fed back into the free layer. The magnetization direction of the free layer determines the resistance of the MTJ as $R = R_{\mathrm{P}} + (\Delta R/2)(1-m_y)$ where R_{P} is the resistance in the parallel state, and ΔR is the difference between the resistances in the antiparallel and parallel states. The oscillations of the free-layer magnetization can be converted into a voltage signal (V_{ac}) by passing a dc current (I_{dc}) through the MTJ given by $V_{\mathrm{ac}} = -(\Delta R/2)m_y I_{\mathrm{dc}}$. Let us denote by R_{W} the resistance of the W wire and denote by R_0 the average resistance of the MTJ, i.e., $R_0 = (R_{\mathrm{P}} + R_{\mathrm{AP}})/2$, where R_{AP} is the resistance of the MTJ in the antiparallel state. The oscillating voltage V_{ac} drives an ac charge current through the W strip given by $I_{\mathrm{ac}} = V_{\mathrm{ac}}/(R_0 + R_{\mathrm{W}})$. The ac charge current converted into an ac spin current via the spin Hall effect is given by $\vec{I}_s = f\,I_{\mathrm{dc}}m_y\hat{y}$, where $f = \theta_{sH}\Delta R L_x/[2t_{\mathrm{W}}(R_0+R_{\mathrm{W}})]$, and θ_{sH} is the spin Hall angle of the of the W wire. This spin current has spins polarized along the y direction and is absorbed by the free layer as it flows along the z direction.

If the delay element introduces a delay of Δt, then the spin current at time t is given by $\vec{I}_s(t) = f\,I_{\mathrm{dc}}m_y(t-\Delta t)\,\hat{y}$. We put this expression into Eq. (1) and assume a small deviation of the magnetization from equilibrium state, i.e., $m_z \cong 1$ and m_x, $m_y \ll 1$. Linearizing Eq. (1), we get the following two equations:

$$\dot{m}_x = -\gamma\,m_y\,(H_\perp + H_{\mathrm{ext}} + H_{//}) - \alpha\gamma\,(H_\perp + H_{\mathrm{ext}})m_x, \tag{3a}$$

$$\dot{m}_y = \gamma\,m_x\,(H_\perp + H_{\mathrm{ext}}) - \alpha\gamma\,m_y(H_\perp + H_{\mathrm{ext}} + H_{//}) + \frac{f I_{\mathrm{dc}} m_y(t-\Delta t)}{qN_s}. \tag{3b}$$

The m_x and m_y in the above equations now represent average values. We assume solutions of the form

$m_x = A\exp(-i\omega t)$, $m_y = B\exp(-i\omega t)$ and put them into the above equations. Note that ω is a complex quantity with a real part ω_R denoting the precessional angular frequency and the imaginary part ω_I denoting the damping. The approximate solutions for ω_R and ω_I are given below:

$$\omega_R \approx \omega_0 + 0.5f\frac{I_{\rm dc}}{qN_s}\sin(\omega_0\Delta t), \tag{4a}$$

$$\omega_I \approx -0.5\left[\alpha\gamma\,(2H_\perp + 2H_{\rm ext} + H_{//}) + f\frac{I_{\rm dc}}{qN_s}\cos(\omega_0\Delta t)\right], \tag{4b}$$

where ω_0 is given by $\omega_0 \approx \gamma\sqrt{(H_{//}+H_{\rm ext}+H_\perp)(H_\perp+H_{\rm ext})}$. We see from Eqs. (3a) and (3b) that both the precession frequency and the damping can be changed by $I_{\rm dc}$ and Δt. If we choose Δt such that $\omega_0\Delta t = (2n+1)\,\pi/2$ where $n = 0$ or a positive integer, the dominant change is in the precessional frequency, but if we choose Δt such that $\omega_0\Delta t = n\pi$, the dominant change is in damping. For a positive value of the dc current (and assuming a positive value of θ_{sH}), an even value of n increases the damping, and an odd value of n decreases the damping. The opposite scenario holds for the negative dc current. The value of the dc current for which the damping becomes zero gives us the critical current, which can be obtained from Eq. (4b). If we choose a value of Δt, such that $\omega_0\Delta t = 2n\pi$ [i.e., $\cos(\omega_0\Delta t) = 1$), the critical current is negative and is given by (for $H_{//} = 0$)

$$I_{\rm dc_{critical}} = -2\alpha\omega_0\frac{t_{\rm W}}{L_x}\frac{2(R_0+R_{\rm W})}{\Delta R}\frac{qN_s}{\theta_{sH}}. \tag{5}$$

If the dc current exceeds the critical current (assuming $H_{\rm ext}$ to be positive), it can be shown by a similar analysis that even the state $m_z = -1$ is unstable. Our numerical analysis of Eq. (1) shows that the free-layer magnetization is driven into precessional states (see Fig. 2). The analytical solution under certain assumptions also shows that precessional states are obtained if the dc current exceeds the critical current (see the Supplemental Material [34]).

III. SIMULATION RESULTS AND DISCUSSION

For a typical MgO-based MTJ, the perpendicular magnetic anisotropy of the free layer can be obtained with $Co_{40}Fe_{40}B_{20}$ with a thickness of 1 nm [31]. We assume a MTJ with 0.9-nm MgO thickness, with TMR = 100%, and RA product = 2 $\Omega\,(\mu{\rm m})^2$. Assuming $L_x = L_y = 100$ nm gives $R_{\rm P} = 200\ \Omega$ and $R_{\rm AP} = 400\ \Omega$. We also use following typical parameters: $M_s = 1000$ emu/cm^3, $\alpha = 0.01$, $\gamma = 2.21\times10^5$ m/(A s), $H_\perp = 1000$ Oe, $H_\parallel = 0$, $\rho_{\rm W} = 21\times10^{-7}\ \Omega$ m, $t_{\rm W} = 9$ nm, $\theta_{sH} = 0.35$, and $\Delta t = 0$. Using these parameters, the critical current comes out to be 60 μA. The LLG equation (1) is integrated numerically including the random magnetic field $\vec{h}_r$. Stratonovich calculus and the Heun scheme are used for the numerical solution [35]. The power spectral density (PSD) of m_y for different values of the dc bias current obtained at 300 K is shown in Fig. 2. The simulations are carried out for 50 μs.

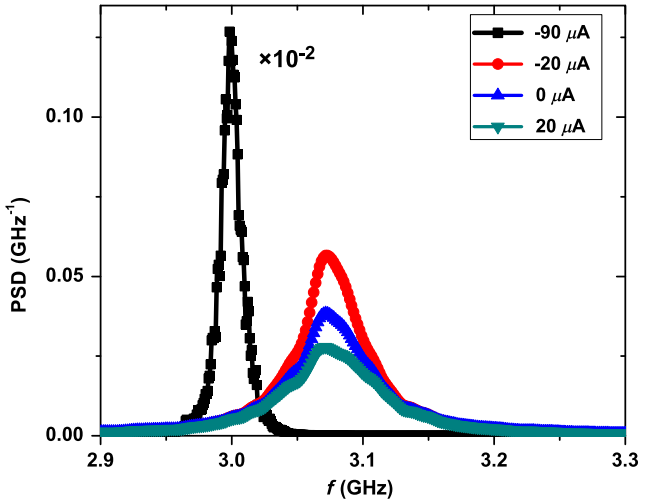

FIG. 2. The PSD of m_y for different dc current values obtained at 300 K. The cyan, blue, and red curves show the PSD for the 20-, 0-, and −20-μA currents, respectively. The damping is enhanced for positive current and reduced for negative current values. The black curve (which is divided by 100 for the sake of clarity) shows the PSD corresponding to the −90-μA current, which is larger than the critical current.

As can be seen from Fig. 2, the spectral density is enhanced for the negative current and reduced for the positive current. This feature is similar to what is observed in the case of spin-transfer-torque-based oscillators driven by current less than the critical current. As the negative current reduces the effective damping, it implies that the effective temperature of the free-layer magnetization increases. This reduction in the damping results in an enhanced PSD for the negative dc current. Similarly, as the effective temperature decreases for the positive current, PSD decreases. A very large spectral density is seen for the −90-μA current, which is greater than the critical current (a delay of 325 ps is used for this calculation).

We also carry out detailed simulations to study the effect of the dc current and delay time on the output power and linewidth of oscillations shown as 2D plots in Figs. 3(a) and 3(b). The power is calculated using the expression $P = [R_L/(R_L + R_{\rm MTJ})^2](0.5\Delta R I_{\rm dc})^2{\rm var}(m_y)$, where R_L is the load resistance taken as 50 Ω, $R_{\rm MTJ}$ is the average resistance of the MTJ, and var denotes variance [16]. The linewidths are extracted by fitting the spectral densities to the Lorentzian function [36]. The linewidth data are then smoothened to obtain the 2D plot.

The output power and linewidth both depend on the current and the delay values. To clarify the 2D plots, we also show some particular cuts in Figs. 3(c) and 3(d).

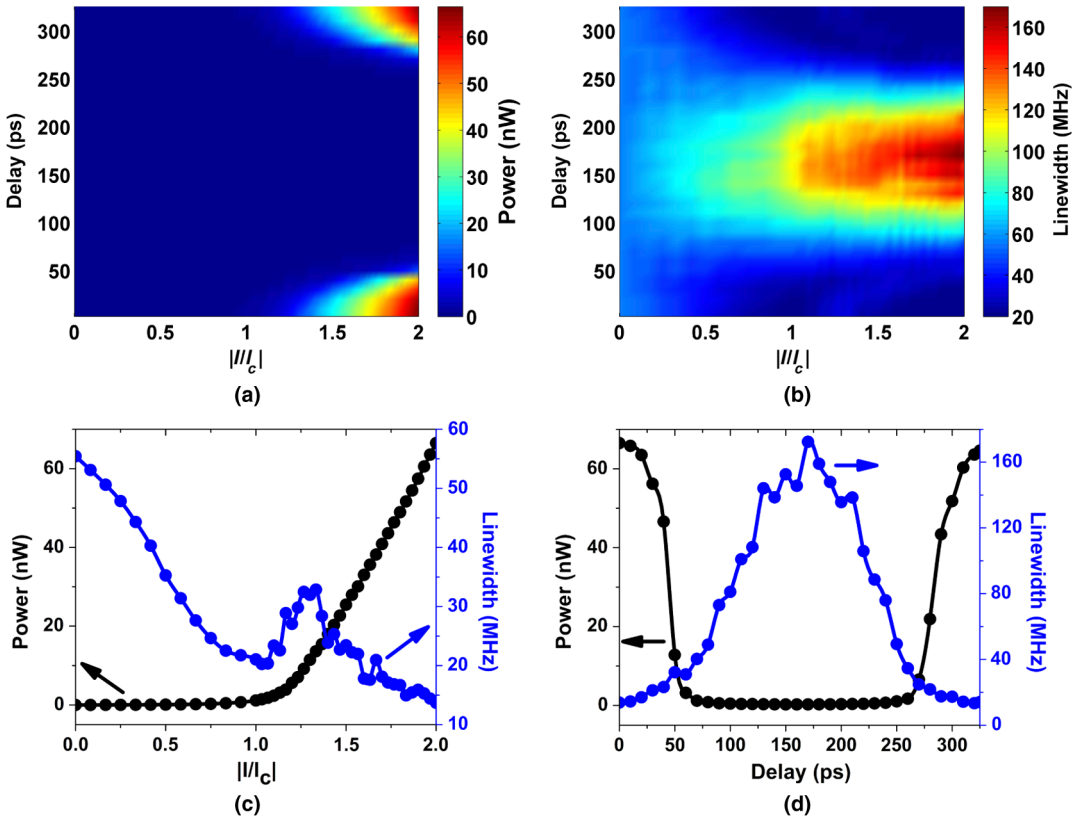

FIG. 3. The output power and linewidth versus dc current and delay-time plots. (a) 2D plot for power, (b) 2D plot for linewidth, (c) power and linewidth variation with current for a particular value of 0-ps delay, and (d) power and linewidth variation with delay for a particular value of the -120-μA current.

Figure 3(c) shows the output power and linewidth as a function of current for a delay of 325 ps. It can be seen that the power increases steeply with the current when it exceeds the critical current. This steep increase is similar to what has been observed in spin-torque oscillators [36,37]. We also calculate the power as a function of the current using a simplified model for the oscillator presented in the Supplemental Material [34]. A similar steep increase in power can be seen in Fig. S1 of the Supplemental Material [34]. The linewidth decreases with the current for small current values. Around the critical current (-60 μA), the linewidth increases and again starts decreasing as the current increases further. This anomalous behavior is a consequence of frequency nonlinearity (dependence of the oscillation amplitude on frequency), something which has been observed experimentally and studied theoretically as well [36–38]. Figure 3(d) shows the output power and linewidth as a function of the delay for the dc current of -120 μA. As explained in the analytical treatment, large magnetization oscillations are possible for phase values of 0 or 2π, and, hence, the output power is maximum when the delay is 0 ps (phase $= 0$) or 325 ps (phase $= 2\pi$) and minimum for intermediate values (phase $= \pi$). Similarly, the linewidth is expected to be less at phase $= 0$ or 2π and larger at intermediate values (π). The linewidth plot in Fig. 3(d) follows this same trend.

The spin current produced due to the dc bias current passing through the pinned layer is neglected in the above simulations. This spin current given by $\vec{I}_s = pI_{\rm dc}\,\hat{m}_{\rm pin}/[1 + p^2(\hat{m}\cdot\hat{m}_{\rm pin})]$, where p is the polarization of the free layer and $\hat{m}_{\rm pin}$ denotes the direction of the pinned layer [1], exerts a spin-transfer torque on the free-layer magnetization. Though this STT does not help in starting the oscillations, once the free layer is set into (large) oscillations by the feedback effect, STT can affect the oscillations. If we include this spin current, we find from the simulations that interplay of the feedback effect and spin current can enhance the amplitude of the oscillations and reduce the linewidth, as shown in Fig. 4.

The effect of spin pumping can be included by assuming an effective value of Gilbert damping, α [7]. A large increase in the damping constant is found in the case of Pt/ferromagnetic (FM) bilayers. However, a large spin-orbit coupling (which leads to large spin Hall angle) does not necessarily imply a large spin-pumping effect, as the spin-pumping effect also depends on other parameters like spin-mixing conductance, etc. [29]. The value of the damping constant (0.01) used in the above simulations is very close to the experimentally observed value in W/CoFeB bilayer (0.0122) [30]. Another important effect to be considered is the fieldlike spin-orbit coupling (also called the Rashba term) [39,40]. The feedback current passing through the FM–heavy-metal layer will give rise to a Rashba magnetic field feedback along the y axis. The effect of this on magnetization dynamics is the same as the oersted-magnetic-field feedback, but the amplitude can be larger.

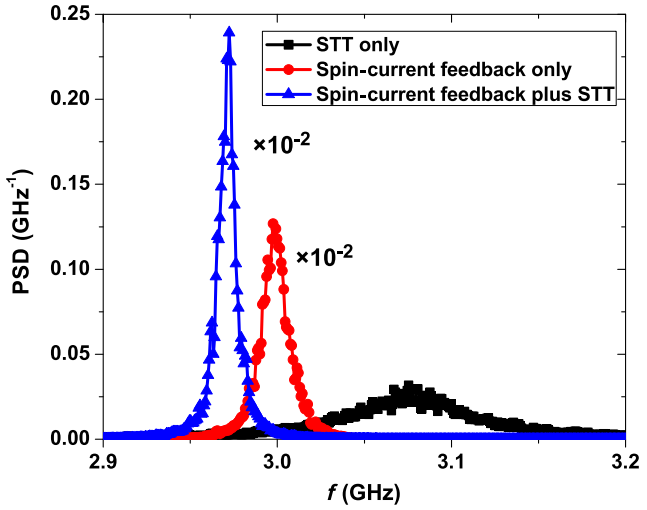

FIG. 4. The PSD plots for the −90-μA current at 300 K of m_y demonstrating the effect of STT generated by the dc bias current. The black, red, and blue curves show the PSD for the case of STT only, spin-current feedback only, and spin-current feedback plus STT considered together. The PSD is much less for the STT-only case and is much larger for the spin-current-feedback-only case (the red and blue curves corresponding to the spin-current-feedback only and spin-current feedback plus STT cases are divided by 100 for the sake of clarity). The enhancement in the PSD and reduction in the linewidth can be seen clearly from the blue curve.

In fact, the Rashba feedback field can be used for inducing oscillations instead of oersted-field feedback. However, for a free layer with only an out-of-plane easy axis as considered in the simulations in this paper, the magnetic field feedback does not lead to stable oscillations. The spin-current feedback via the spin Hall effect, on the other hand, leads to stable precessional states (see the Supplemental Material [34]). Though the magnetic field feedback cannot be used for stable precession here, for low values of feedback, it changes the damping. It should be further noted that for spin-current feedback, condition $\omega_0 \Delta t = n\pi$ changes the damping, whereas for magnetic field feedback, the condition for change in damping is $\omega_0 \Delta t = (2n+1)\pi/2$. This is due to the different symmetry of STT and magnetic field torque [41].

IV. COUPLED-MAGNET OSCILLATOR

We now consider a system of two nanomagnets coupled via magnetic dipolar interaction. We show that the different oscillation modes of this system can be excited by using the spin-current-feedback scheme. The schematic diagram for the experimental realization is shown in Fig. 5. FM1 and FM2 are electrically isolated by a thick insulator so that the dc bias current passes only through the top MTJ.

As in the previous case, the magnetization direction fluctuations of FM1 drive a charge current in the W wire, which converts it into spin current by the spin Hall effect.

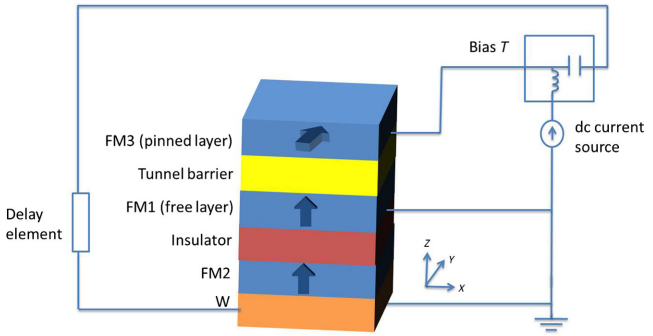

FIG. 5. Schematic diagram of the proposed spintronic oscillator. The top layer (FM3) is again pinned along the y axis, and the bottom layer (FM1) is the free layer with easy axis out-of-plane. The free layer is dipole coupled to another nanomagnet (FM2). FM2 rests on top of a W wire and is electrically isolated from the MTJ. The fluctuations of FM1 drive fluctuating current through the W strip, which is converted into spin current via the spin Hall effect and fed into the FM2 layer. The phase of the feedback can be adjusted to amplify different modes of the dipole-coupled FM1-FM2 system.

The difference from the previous case is that the spin current is fed back into FM2, rather than FM1. As the FM2 is dipole coupled with FM1, the feedback spin current affects the dynamics of both nanomagnets. Assuming $m_{1z} \cong 1$, $m_{2z} \cong 1$, and small oscillations, the linearized LLGS equations in this case can be written as

$$\dot{m}_{1x} = -\gamma\, m_{1y}\,(H_{//} + H_{\rm ext} + H_3 + H_\perp) - \alpha\gamma\,(H_\perp + H_{\rm ext}) m_{1x} - \gamma H_2 m_{2y} - \alpha\gamma\, H_1 m_{2x}, \quad (6a)$$

$$\dot{m}_{1y} = \gamma\, m_{1x}\,(H_\perp + H_{\rm ext} + H_3) - \alpha\gamma\, m_{1y}(H_{//} + H_{\rm ext} + H_\perp) + \gamma H_1 m_{2x} - \alpha\gamma H_2 m_{2y}, \quad (6b)$$

$$\dot{m}_{2x} = -\gamma\, m_{2y}\,(H_{//} + H_{\rm ext} + H_3 + H_\perp) - \alpha\gamma\,(H_\perp + H_{\rm ext}) m_{2x} - \gamma H_2 m_{1y} - \alpha\gamma H_1 m_{1x}, \quad (6c)$$

$$\dot{m}_{2y} = \gamma\, m_{2x}\,(H_\perp + H_{\rm ext} + H_3) - \alpha\gamma\, m_{2y}(H_{//} + H_{\rm ext} + H_\perp) + \gamma H_1 m_{1x} - \alpha\gamma H_2 m_{1y} + \frac{f I_{\rm dc} m_{1y}(t-\Delta t)}{q N_s}, \quad (6d)$$

where the indices 1 and 2 are for magnet 1 and magnet 2, respectively. We assume both magnets have identical dimensions and parameters such as α, γ, $H_{//}$, and $H_\perp$, H_1, H_2, H_3 (all three positive) denote the coupling between them, e.g., the dipolar magnetic field acting on FM1 from FM2 is given by $\vec{H} = -H_1 m_{2x}\hat{x} - H_2 m_{2y}\hat{y} + H_3 m_{2z}\hat{z}$, where $H_1 + H_2 = H_3$. (This relation means that the trace of the demagnetization tensor is 0 [42]). A similar relation holds for the dipolar field acting on FM2. The spin current due to the flow of dc current through the fixed layer is neglected, as done for Eqs. (3a) and (3b). The last term in

Eq. (6d) is due to the spin-current feedback and depends on the y component of the magnetization of FM1 at time t-Δt. Now we analyze above equations assuming $H_{//} = 0$ for simplicity. We also assume $L_x = L_y$, which implies $H_1 = H_2$. Let us first take the case where the feedback term is not present. The system of coupled nanomagnets then has two resonant modes with angular frequencies given by $\omega_{01} = \gamma(H_{\rm ext} + H_\perp + H_3 - H_1)$ and $\omega_{02} = \gamma(H_{\rm ext} + H_\perp + H_3 + H_1)$. The higher-frequency mode corresponds to in-phase oscillations, and the lower-frequency mode corresponds to 180° out-of-phase oscillations of FM1 and FM2. Let us now include the spin-current feedback, i.e., the last term in Eq. (6d). Following a similar analysis as is done for Eqs. (3a) and (3b), we can determine the effect of the spin-current feedback on these two modes. It turns out that if we choose the delay such that $\omega_0 \Delta t = n\pi$, the dominant change is in the damping of the mode, and if $\omega_0 \Delta t = (2n+1)\pi/2$, the dominant change is in the frequency of the mode, where $n = 0$ or a positive integer, and ω_0 refers to either ω_{01} or ω_{02}. Interestingly, if we choose $\omega_0 \Delta t = 2n\pi$, the positive dc bias current increases the damping of the low-frequency mode and decreases the damping of the high-frequency mode. The opposite scenario holds for $\omega_0 \Delta t = (2n+1)\pi$. Thus, if we choose $\Delta t = 0$, the positive current increases the damping of the low-frequency mode and decreases the damping of the high-frequency mode (the opposite scenario for negative current). In other words, if we pass a large positive current, the system of coupled magnets will undergo precessional motion as the damping of the high-frequency mode becomes negative. If we pass large negative current, the system again undergoes precession as the damping of the low-frequency mode becomes negative. The expression for the magnitude of the critical current is given by

$$I_{\rm dc_{critical}} = 4\alpha\omega_0 \frac{t_{\rm W}}{L_x} \frac{2(R_0 + R_{\rm W})}{\Delta R} \frac{qN_s}{\theta_{sH}}. \qquad (7)$$

Equation (7) shows that the critical current for the coupled-magnet system is twice that of the single-magnet case [see Eq. (5)], as we are driving two magnets into precessional modes.

The power spectral density of the y component of magnetization of the FM1 obtained from the numerical solution of the coupled magnet system is shown in Fig. 5. We use the same values of the parameters used for the single-magnet case. Assuming a 10-nm-thick insulator between FM1 and FM2, the dipolar couplings H_1, H_2, and H_3 are estimated to be 35, 35, and 70 Oe, respectively [42]. The two peaks in blue in Fig. 6 obtained for zero dc bias current show the two resonant frequencies. When a bias current of -30 μA is passed ($\Delta t = 0$), the low-frequency peak is enhanced, and the high-frequency peak is suppressed. The opposite scenario is obtained for the positive current, in agreement with the above discussion.

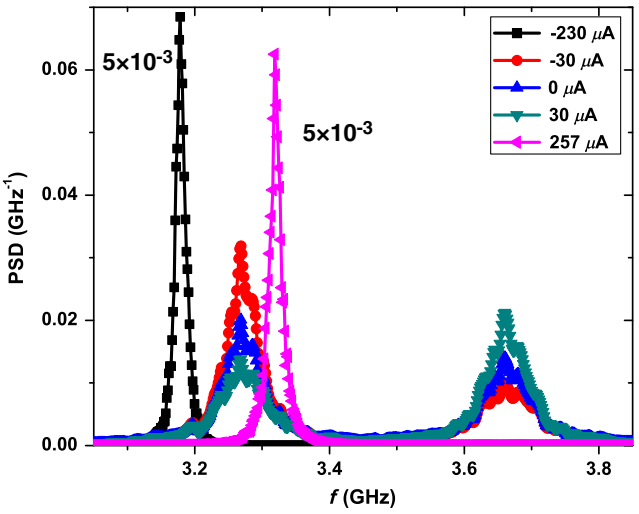

FIG. 6. The spectral density of m_y for different dc current values for the coupled-magnets case obtained at 300 K. The red, blue, and cyan curves show the PSD for the −30-, 0-, and 30-μA currents, respectively. The low-frequency peak is enhanced for negative current values, and the high-frequency peak is enhanced for positive current values. The black and pink curves show the PSD for a large negative current (−230 μA) and a large positive current (257 μA). For the sake of clarity, the PSDs corresponding to the −230- and 257-μA currents are divided by 200.

For larger positive and negative currents exceeding the critical currents, precessional states are obtained which give rise to large and sharp peaks in the spectral density.

V. CONCLUSIONS

In summary, we show that spin-current feedback can be used to drive a nanomagnet into precessional states. This scheme is useful for a rf oscillator based on a MTJ with an in-plane fixed layer and an out-of-plane magnetized free layer. The critical current depends inversely on the spin Hall angle of the material used [see Eq. (5) or (7)]. The critical current can be reduced by using materials with giant spin Hall effect [32,33]. The future research will involve the experimental demonstration of the proposed designs.

ACKNOWLEDGMENTS

We are thankful to the Centre of Excellence in Nanoelectronics at the IIT-Bombay Nanofabrication Facility and Department of Electronics and Information Technology, Government of India for its support. We acknowledge Professor Y. Suzuki, Osaka University for useful discussions.

[1] J. C. Slonczewski, Current-driven excitation of magnetic multilayers, J. Magn. Magn. Mater. **159**, L1 (1996).

[2] L. Berger, Emission of spin waves by a magnetic multilayer traversed by a current, Phys. Rev. B **54**, 9353 (1996).
[3] J. A. Katine, F. J. Albert, R. A. Buhrman, E. B. Myers, and D. C. Ralph, Current-Driven Magnetization Reversal and Spin-Wave Excitations in Co/Cu/Co Pillars, Phys. Rev. Lett. **84**, 3149 (2000).
[4] E. B. Myers, D. C. Ralph, J. A. Katine, R. N. Louie, and R. A. Buhrman, Current-induced switching of domains in magnetic multilayer devices, Science **285**, 867 (1999).
[5] S. I. Kiselev, J. C. Sankey, I. N. Krivorotov, N. C. Emley, R. J. Schoelkopf, R. A. Buhrman, and D. C. Ralph, Microwave oscillations of a nanomagnet driven by a spin-polarized current, Nature (London) **425**, 380 (2003).
[6] H. Kubota, A. Fukushima, Y. Ootani, S. Yuasa, K. Ando, H. Maehara, K. Tsunekawa, D. D. Djayaprawira, N. Watanabe, and Y. Suzuki, Evaluation of spin-transfer switching in CoFeB/MgO/CoFeB magnetic tunnel junctions, Jpn. J. Appl. Phys. **44**, L1237 (2005).
[7] D. C. Ralph and M. D. Stiles, Spin transfer torques, J. Magn. Magn. Mater. **320**, 1190 (2008).
[8] A. Bose, A. K. Shukla, K. Konishi, S. Jain, N. Asam, S. Bhuktare, H. Singh, D. D. Lam, Y. Fujii, S. Miwa, Y. Suzuki, and A. A. Tulapurkar, Observation of thermally driven field-like spin torque in magnetic tunnel junctions, Appl. Phys. Lett. **109**, 032406 (2016).
[9] Z. Zeng, G. Finocchio, and H. Jiang, Spin transfer nano-oscillators, Nanoscale **5**, 2219 (2013).
[10] S. E. Russek, W. H. Rippard, T. Ceciland, and R. Heindl, in *Spin-Transfer Nano-Oscillators, Handbook of Nano Physics*, edited by K. D. Sattler (CRC press, Taylor & Francis group, Boca Raton, 2010).
[11] A. M. Deac, A. Fukushima, H. Kubota, H. Maehara, Y. Suzuki, S. Yuasa, Y. Nagamine, K. Tsunekawa, D. D. Djayaprawira, and N. Watanabe, Bias-driven large power microwave emission from MgO-based tunnel magneto-resistance devices, Nat. Phys. **4**, 803 (2008).
[12] W. H. Rippard, M. R. Pufall, S. Kaka, T. J. Silva, and S. E. Russek, Current-driven microwave dynamics in magnetic point contacts as a function of applied field angle, Phys. Rev. B **70**, 100406R (2004).
[13] F. B. Mancoff, N. D. Rizzo, B. N. Engel, and S. Tehrani, Phase-locking in double-point-contact spin-transfer devices, Nature (London) **437**, 393 (2005).
[14] S. Sharma, B. Muralidharan, and A. Tulapurkar, Proposal for a domain wall nano-oscillator driven by non-uniform spin currents, Sci. Rep. **5**, 14647 (2015).
[15] D. Dixit, K. Konishi, C. V. Tomy, Y. Suzuki, and A. A. Tulapurkar, spintronic oscillator based on magnetic field feedback, Appl. Phys. Lett. **101**, 122410 (2012).
[16] Dinesh Kumar, K. Konishi, Nikhil Kumar, S. Miwa, A. Fukushima, K. Yakushiji, S. Yuasa, H. Kubota, C. V. Tomy, A. Prabhakar, Y. Suzuki, and A. Tulapurkar, Coherent microwave generation by spintronic feedback oscillator, Sci. Rep. **6**, 30747 (2016).
[17] K. J. Lee, O. Redon, and B. Dieny, Analytical investigation of spin-transfer dynamics using a perpendicular-to-plane polarizer, Appl. Phys. Lett. **86**, 022505 (2005).
[18] D. Houssameddine, U. Ebels1, B. Delaet, B. Rodmacq, I. Firastrau, F. Ponthenier, M. Brunet, C. Thirion, J.-P. Michel, L. Prejbeanu-Buda, M. C. Cyrille, O. Redon, and B. Dieny, Spin-torque oscillator using a perpendicular polarizer and a planar free layer, Nat. Mater. **6**, 447 (2007).
[19] V. S. Tiberkevich, R. S. Khymyn, H. X. Tang, and A. N. Slavin, Sensitivity to external signals and synchronization properties of a non-isochronous auto-oscillator with delayed feedback, Sci. Rep. **4**, 3873 (2014).
[20] Guru Khalsa, M. D. Stiles, and J. Grollier, Critical current and linewidth reduction in spin-torque nano-oscillators by delayed self-injection, Appl. Phys. Lett. **106**, 242402 (2015).
[21] S. Tsunegi, E. Grimaldi, R. Lebrun, H. Kubota, A. S. Jenkins, K. Yakushiji, A. Fukushima, P. Bortolotti, J. Grollier, S. Yuasa, and V. Cros, Self-injection locking of a vortex spin torque oscillator by delayed feedback, Sci. Rep. **6**, 26849 (2016).
[22] M. I. D'yakonov and V. I. Perel, Possibility of orienting electron spins with current, JETP Lett. **13**, 467 (1971) [Sov. Phys. JETP **33**, 467 (1971)].
[23] J. E. Hirsch, Spin Hall Effect, Phys. Rev. Lett. **83**, 1834 (1999).
[24] Y. K. Kato, R. S. Myers, A. C. Gossard, and D. D. Awschalom, Observation of the spin Hall effect in semiconductors, Science **306**, 1910 (2004).
[25] T. Kimura, Y. Otani, T. Sato, S. Takahashi, and S. Maekawa, Room-Temperature Reversible Spin Hall Effect, Phys. Rev. Lett. **98**, 156601 (2007).
[26] E. Saitoh, M. Ueda, H. Miyajima, and G. Tatara, Conversion of spin current into charge current at room temperature: Inverse spin-Hall effect, Appl. Phys. Lett. **88**, 182509 (2006).
[27] O. Mosendz, V. Vlaminck, J. E. Pearson, F. Y. Fradin, G. E. W. Bauer, S. D. Bader, and A. Hoffmann, Detection and quantification of inverse spin Hall effect from spin pumping in permalloy/normal metal bilayers, Phys. Rev. B **82**, 214403 (2010).
[28] L. Liu, T. Moriyama, D. C. Ralph, and R. A. Buhrman, Spin-Torque Ferromagnetic Resonance Induced by the Spin Hall Effect, Phys. Rev. Lett. **106**, 036601 (2011).
[29] L. Liu, C. F. Pai, Y. Li, H. W. Tseng, D. C. Ralph, and R. A. Buhrman, Spin-torque switching with the giant spin Hall effect of tantalum, Science **336**, 555 (2012).
[30] C. F. Pai, L. Liu, Y. Li, H. W. Tseng, and D. C. Ralph, Spin transfer torque devices utilizing the giant spin Hall effect of tungsten, Appl. Phys. Lett. **101**, 122404 (2012).
[31] Q. Hao and G. Xiao, Giant Spin Hall Effect and Switching Induced by Spin-Transfer Torque in a $W/Co_{40}Fe_{40}B_{20}/MgO$ Structure with Perpendicular Magnetic Anisotropy, Phys. Rev. Applied **3**, 034009 (2015).
[32] J. Sinova, S. O. Valenzuela, J. Wunderlich, C. H. Back, and T. Jungwirth, Spin Hall effects, Rev. Mod. Phys. **87**, 1213 (2015).
[33] G. Vignale and J. Supercond, Ten years of spin Hall effect, J. Supercond. Novel Magn. **23**, 3 (2010).
[34] See Supplemental Material at http://link.aps.org/supplemental/10.1103/PhysRevApplied.7.014022 for analytical solutions of the precessional states obtained by spin-current and magnetic field feedback, a comparison between them, and output power variation with current obtained from analytical treatment.

[35] J. L. Garcia-Palacios and F. J. Lazaro, Langevin-dynamics study of the dynamical properties of small magnetic particles, Phys. Rev. B **58**, 14937 (1998).

[36] A. Slavin and V. Tiberkevich, Nonlinear auto-oscillator theory of microwave generation by spin-polarized current, IEEE Trans. Magn. **45**, 1875 (2009).

[37] Q. Mistral, J. Kim, T. Devolder, P. Crozat, C. Chappert, J. A. Katine, M. J. Carey, and K. Ito, Current-driven microwave oscillations in current perpendicular-to-plane spin-valve nanopillars, Appl. Phys. Lett. **88**, 192507 (2006).

[38] J. Kim, Q. Mistral, C. Chappert, V. Tiberkevich, and A. Slavin, Line Shape Distortion in a Nonlinear Auto-Oscillator Near Generation Threshold: Application to Spin-Torque Nano-Oscillators, Phys. Rev. Lett. **100**, 167201 (2008).

[39] I. M. Miron, G. Gaudin, S. Auffret, B. Rodmacq, A. Schuhl, S. Pizzini, J. Vogel, and P. Gambardella, Current-driven spin torque induced by the Rashba effect in a ferromagnetic metal layer, Nat. Mater. **9**, 230 (2010).

[40] K. Garello, I. M. Miron, C. O. Avci, F. Freimuth, Y. Mokrousov, S. Blugel, S. Auffret, O. Boulle, G. Gaudin, and P. Gambardella, Symmetry and magnitude of spin–orbit torques in ferromagnetic heterostructures, Nat. Nanotechnol. **8**, 587 (2013).

[41] A. A. Tulapurkar, Y. Suzuki, A. Fukushima, H. Kubota, H. Maehara, K. Tsunekawa, D. D. Djayaprawira, N. Watanabe, and S. Yuasa, Spin-torque diode effect in magnetic tunnel junctions, Nature (London) **438**, 339 (2005).

[42] A. J. Newell, W. Williams, and D. J. Dunlop, A generalization of the demagnetizing tensor for nonuniform magnetization, J. Geophys. Res. **98**, 9551 (1993).